BASIC RESEARCH IN WAKE VORTEX ALLEVIATION

USING A VARIABLE TWIST WING

By Dana J. Morris and G. Thomas Holbrook
NASA Langley Research Center

INTRODUCTION

Aircraft trailing vortices are one of the principal factors affecting aircraft acceptance and departure rates at airports. Minimization of the hazard posed by the vortex would allow reduction of the present spacing requirements. Such reductions would allow full utilization of advances in automatically aided landing systems while maintaining or improving safety within the terminal area. For several years, NASA has been conducting an in-house and contractual research effort involving theoretical and experimental studies of various wake vortex minimization techniques (refs. 1 and 2). This work was done in conjunction with the Federal Aviation Administration's investigation of various sensing devices for detecting the presence of vortices within the terminal area.

This work has identified several methods of reducing the vortex strength behind an aircraft. These involve the redistribution of lift (vorticity) spanwise on the wing and drag (turbulence) distribution along the wing. NASA's continued effort involves experiments and theoretical analysis aimed at improving the understanding of the physics of vortex dissipation. This report summarizes one area of NASA's basic research in wake vortex alleviation and contains the highlights of model tests using a variable twist wing to investigate various wing span-load and drag distributions.

SYMBOLS

All force and moment data are referenced to the wind axes.

b reference wing span, m

$\bar{c}$ wing mean aerodynamic chord, m

c_l sectional lift coefficient

C_D drag coefficient, $\frac{\text{Drag force}}{q_\infty S}$

C_L lift coefficient, $\frac{\text{Lift force}}{q_\infty S}$

C_l trailing-wing rolling-moment coefficient, $\frac{\text{Rolling moment}}{q_\infty S b}$

C_p pressure coefficient, $\frac{p - p_\infty}{q_\infty}$

P static pressure, Pa

q dynamic pressure, Pa

S reference wing area, m^2

u component of velocity parallel to the x-axis, m/sec

V resultant velocity magnitude, m/sec

VTW refers to Variable Twist Wing

v component of velocity parallel to the y-axis, m/sec

w component of velocity parallel to the z-axis, m/sec

x longitudinal axis referenced to Variable Twist Wing centerline, positive aft, m

y lateral axis referenced to Variable Twist Wing centerline, positive out right wing, m

z vertical axis referenced to Variable Twist Wing quarter-chord line, positive above wing, m

$\Delta\alpha$ wing-segment twist angle relative to wing center panel, wing leading edge up is positive, deg

η vorticity, counterclockwise flow is positive, per sec

Subscripts:

TW refers to trailing wing

VTW refers to Variable Twist Wing

∞ refers to free-stream conditions

TEST FACILITIES

The tests were conducted in the Langley V/STOL Tunnel and, under contract, in the Hydronautics Ship Model Basin.

V/STOL Wind Tunnel

The test section of the V/STOL tunnel has a height of 4.42 m, a width of 6.63 m, and a length of 14.24 m. The Variable Twist Wing was blade mounted and maintained at 2.2 m above the test section floor (floor-to-wing center panel trailing edge) during test runs. Angle of attack was determined from an

accelerometer mounted in the fuselage (ref. 3). A six-component strain-gage balance measured lift, drag, and pitching-moment data.

A survey rig (see fig. 1) was utilized in these tests for crossplane sampling of the three wake velocity components or rolling moment on a trailing wing in the wake of the Variable Twist Wing. The survey rig could be positioned anywhere from 1.2 m to 13.7 m downstream of the wing. The appropriate sensor was mounted to a motor-driven traverse mechanism on the survey rig to allow moving the sensor both laterally and vertically. Digital encoders on the mechanism output the lateral and vertical position of the sensor during test runs.

Hydronautics Ship Model Basin

The Hydronautics Ship Model Basin is a water tank 125 m long and 7.3 m wide, with a water depth of 3.8 m. Two independently powered carriage systems propel the Variable Twist Wing and trailing wing down the tank (see fig. 2). The Variable Twist Wing was located 0.56 span below the water line and attached to the lead carriage by a strut mounted to a tilt table. The tilt table provided for angle-of-attack adjustment (ref. 3). Balances internal to the model center body measured lift, drag, and pitching-moment data.

The trailing-wing carriage has a motor-driven vertical-scan system allowing a 0.46-m vertical survey of the wake during runs at a scanning rate of 0.04 m/sec. The lateral position of the trailing wing is changed manually between runs. The separation distance between the two models was determined using the time differential for the two carriages to pass a point half-way down the tow tank and the measured speed of the carriages.

MODELS

Variable Twist Wing

The Variable Twist Wing (VTW), shown in figure 3, is a unique research model capable of generating a desired span loading by twisting spanwise wing segments to the proper local angle of attack. In this manner, the effect of highly varied span loadings on the rolled-up wake can be investigated. The effect of turbulence on the rolled-up wake can be determined from tests made with various turbulence injection devices attached to the VTW model.

The aspect-ratio 7 metal wing has a span of 2.489 m. As shown in figure 4, the fixed 0.35-m center span is bounded on each end by 36 independently movable sections, each about 0.03 m wide. The 20 instrumented spanwise locations, each with 29 pressure ports, were electronically scanned and recorded in about one-tenth of a second to obtain pressure coefficient data, C_p, during tests in the V/STOL tunnel.

Trailing Wing

Rolling moment on a smaller trailing wing has been used as a means of estimating the hazard posed by a vortex wake system. The aspect-ratio 5.35 trailing wing used for these tests has a span 13 percent of the VTW span. A photograph and dimensions of the unswept trailing-wing model installed on the V/STOL survey rig are presented in figure 5. In each test facility, the model was mounted on a roll balance and attached to a traverse mechanism capable of positioning the model both laterally and vertically in the VTW wake. The model and its roll-balance system were used to measure the rolling moment caused by the vortex flow downstream of the VTW model.

METHOD OF TESTING AND ANALYSIS

The tests were all made at a Variable Twist Wing C_L of 0.6 and a Reynolds number of about one million, based on wing chord. A matrix of the configurations tested is shown in table I. Figure 6 shows schematically the types of data taken at the different downstream locations.

Lift distributions for each configuration tested in the V/STOL tunnel were calculated from the measured C_p data. During the tests, an on-line computer program utilized about half the pressure port data to produce rough plots of spanwise loading. This enabled "fine tuning" of the VTW twist distribution to match the desired loading.

Force and moment data (lift, drag, and pitching-moment) on the Variable Twist Wing were taken throughout an angle-of-attack range in the V/STOL tunnel. Generally, only the force and moment data necessary to assure testing at $C_{L_{VTW}} = 0.6$ were taken in the water towing tank.

Measured trailing-wing rolling-moment coefficients given in this report represent an averaged $C_{l_{TW}}$ for V/STOL data and a peak $C_{l_{TW}}$ for the water-tank data. The V/STOL technique for measuring rolling moment is to position the probe and take 10 data points per second over a 5-second period. These data points are averaged and used as the $C_{l_{TW}}$ for that y,z location. Data are taken at a sufficient number of y,z positions to insure location of the position of the maximum $C_{l_{TW}}$ value obtained by this method. The Hydronautics technique for measuring rolling moment uses the probe to traverse the wake vertically for a single lateral position. Sufficient runs are made at different probe lateral positions to insure locating the y,z position for the peak $C_{l_{TW}}$. The Hydronautics measured $C_{l_{TW}}$ thus represents the maximum instantaneous value of rolling moment obtained in the y,z crossplane of the wake. On several VTW configurations, multiple vortices were shed from each wing semispan. Only the maximum strength vortex is noted in this report.

Three-component wake velocity measurements were made using a three-component hot-film probe, mounted in the V/STOL survey rig. Hot-film voltages

and y,z potentiometer outputs from the traverse mechanisms were signal conditioned and recorded on magnetic tape. This tape was digitized to a matrix of y, z, u, v, and w data values over a 1.524 m × 1.524 m, 0.0254-m mesh, crossplane grid. Vorticity contours were computed from the crossplane velocities at each of the downstream data stations. Comparison of velocity and vorticity plots at the downstream sampling planes shows the development of the wake. Additionally, the data from the half-span downstream station were used as initial conditions for the two-dimensional, time marching, viscous wake simulation computer code (WAKE). (See ref. 4.)

RESULTS

Data were taken at the discrete locations shown in table I and all the data curves shown are faired through these data points. Among the tests (table I) were three relatively simple VTW loadings, each of which resulted in a rolled-up wake with one significant strength semispan vortex. These three configurations (1, 2, and 4) and their measured $C_{l_{TW}}$ values are compared in figure 7. The comparative values of $C_{l_{TW}}$ are as expected, with the simulated rectangular (2) loading generating the maximum rolling moment and the simulated triangular (4) loading creating the minimum. The relative relationship of $C_{l_{TW}}$ data for configurations 1 and 4 also agrees between test facilities. Thus, up to a 30-percent reduction in trailing-wing rolling moment can be achieved in a single semispan vortex wake by span-load alteration on the generating wing. Turbulence differences are considered to be insignificant since the C_D is nearly identical for the three configurations at a C_L of 0.6.

The lift distribution for configuration 7 is similar to that of an 80-percent flapped wing and results in a downstream semispan wake composed of an inboard, or flap, vortex and an outboard, or wingtip, vortex. For this configuration, the flap vortex is highly dominant - in the V/STOL tunnel, the wake velocity data indicate vorticity levels for the flap vortex are at least 30 percent greater than those for the wingtip vortex at 3 spans downstream and, in the water tank, $C_{l_{TW}}$ for the flap vortex was measured as 60 percent greater than the wingtip vortex. Addition of a spoiler centered at $0.61(b_{VTW}/2)$ (configuration 7S) results in a far downstream semispan wake with only one vortex and, as shown in figure 8, a significantly lower $C_{l_{TW}}$. It is important to note that the lift distribution for configuration 7S varies greatly from that of configuration 7, as does the turbulence distribution (evidenced by a 230-percent increase in C_D for configuration 7S at a C_L of 0.6). Therefore, the reduction in measured $C_{l_{TW}}$ may result from the modified lift and turbulence distributions, the increased turbulence level, or a combination of these factors.

In an effort to separate the effect of turbulence from that of span load, the VTW was adjusted (configuration 9) to match the span load of configuration 7 with the spoiler (configuration 7S). Figure 10 compares configurations 7, 7S, and 9. It is apparent that configuration 9 does not achieve the complete

$C_{l_{TW}}$ reduction between configurations 7 and 7S. In fact, the V/STOL tunnel data, for $x/b_{VTW} < 5.5$, show a large increase in $C_{l_{TW}}$ for configuration 9 as opposed to configuration 7. However, at an x/b_{VTW} of 35, the water-tank data indicate an 11-percent reduction in $C_{l_{TW}}$ from configuration-7 values as opposed to an overall 32-percent reduction between configurations 7 and 7S. Thus, it seems that one-third of the measured $C_{l_{TW}}$ reduction between configurations 7 and 7S may be accounted for by span-load alteration - the remainder occurring due to turbulence distribution and level changes.

The nondimensional vorticity contours for configuration 7S are shown in figure 11. The four vortices present one-half span behind the wing have merged into two vortices by five-and-one-half spans downstream. The measured values at the half-span station were used to initialize the WAKE code to predict the development downstream. The vorticity contours predicted by WAKE at five-and-one-half spans downstream are shown in figure 12 for comparison with the measured values shown in figure 11(c). While the predicted vorticity levels are higher than those measured, the locations and shapes of the contours are approximately the same.

CONCLUDING REMARKS

The Variable Twist Wing concept has been used to investigate the relative effects of lift and turbulence distributions on the rolled-up vortex wake. The extensive data gathered will assist in understanding the development and decay of the wake. Also, initial attempts to use the Variable Twist Wing velocity data to validate the WAKE computer code have shown a strong correlation, although the vorticity levels were not exactly matched. Further data analysis and verification of the computer code is proceeding.

REFERENCES

1. Wake Vortex Minimization. NASA SP-409, 1976.

2. Proceedings of the Aircraft Wake Vortices Conference. March 15-17, 1977. Report No. FAA-RD-77-68.

3. Stickle, Joseph W.; and Kelly, Mark W.: Ground-Based Facilities for Evaluating Vortex Minimization Concepts. Wake Vortex Minimization. NASA SP-409, 1977, pp. 129-155.

4. Bilanin, Alan E.; Hirsh, Joel E.; Teske, Milton E.; and Hecht, Arthur M.: Atmospheric-Wake Vortex Interactions. ARAP Report No. 331, 1978.

TABLE I.- DATA TAKEN WITH THE VARIABLE TWIST WING

Designation	Description of wing loading or configuration being simulated	Test facility		Type of data								
		V/STOL	Hydronautics	Force and moment	C_p	$C_{l_{TW}}$, x/b_{VTW} =				u,v,w; x/b_{VTW} =		
						3.0	5.5	20.	35.	0.5	3.0	5.5
1	Straight wing	✓		✓	✓	✓	✓					
1	Straight wing		✓	✓			✓	✓	✓			
2	Rectangular loading	✓		✓	✓	✓	✓					
3	Parabolic loading	✓		✓	✓	✓	✓					
4	Triangular loading	✓		✓	✓	✓	✓			✓	✓	✓
4	Triangular loading		✓	✓			✓	✓	✓			
5	Flapped wing to 40% semispan	✓		✓	✓	✓	✓					
6	Flapped wing to 60% semispan	✓		✓	✓	✓	✓					
7	Flapped wing to 80% semispan	✓		✓	✓	✓	✓			✓	✓	✓
7	Flapped wing to 80% semispan		✓	✓			✓	✓	✓			
7S	Configuration 7 with spoiler centered at $0.6l(b_{VTW}/2)$	✓		✓	✓	✓	✓			✓	✓	✓
7S	Configuration 7 with spoiler centered at $0.6l(b_{VTW}/2)$		✓	✓			✓	✓	✓			
7X	Configuration 7 with spline centered at $0.6l(b_{VTW}/2)$		✓	✓			✓	✓	✓			
8	Twisted wing simulation of 7S lift distribution	✓		✓	✓	✓	✓					
8.5	Twisted wing simulation of 7S lift distribution	✓		✓	✓	✓	✓			✓	✓	✓
8.5X	Configuration 8.5 with flat plate aft of wing centered at $0.6l(b_{VTW}/2)$	✓		✓	✓		✓					
9	Twisted wing simulation of 7S lift distribution	✓		✓	✓	✓	✓					
9	Twisted wing simulation of 7S lift distribution		✓	✓			✓	✓	✓			
9X	Configuration 9 with spline centered at $0.6l(b_{VTW}/2)$		✓	✓			✓	✓	✓			

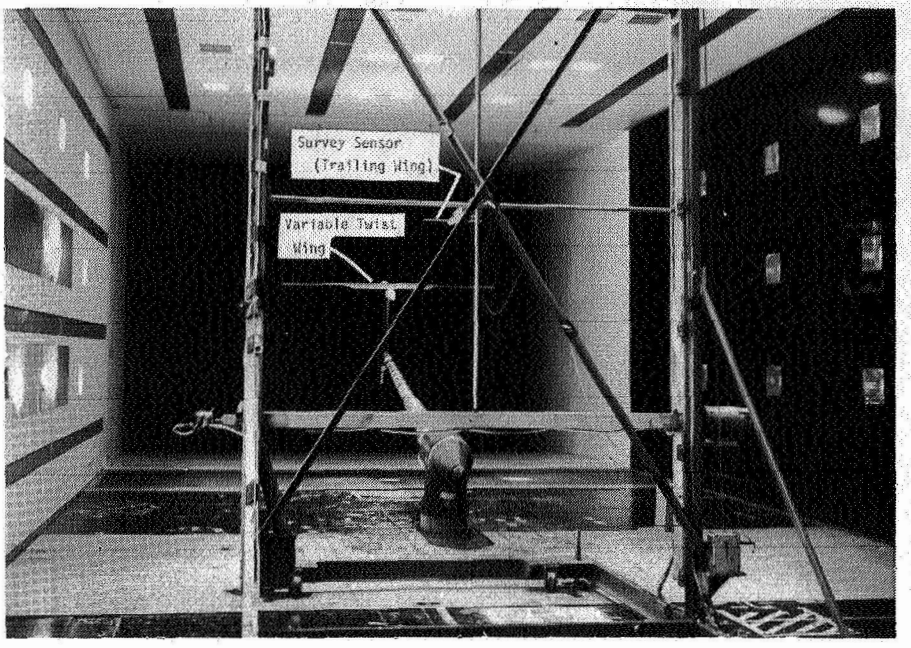

Figure 1.- Survey rig in Langley V/STOL Tunnel (with trailing-wing model attached to traverse mechanism.

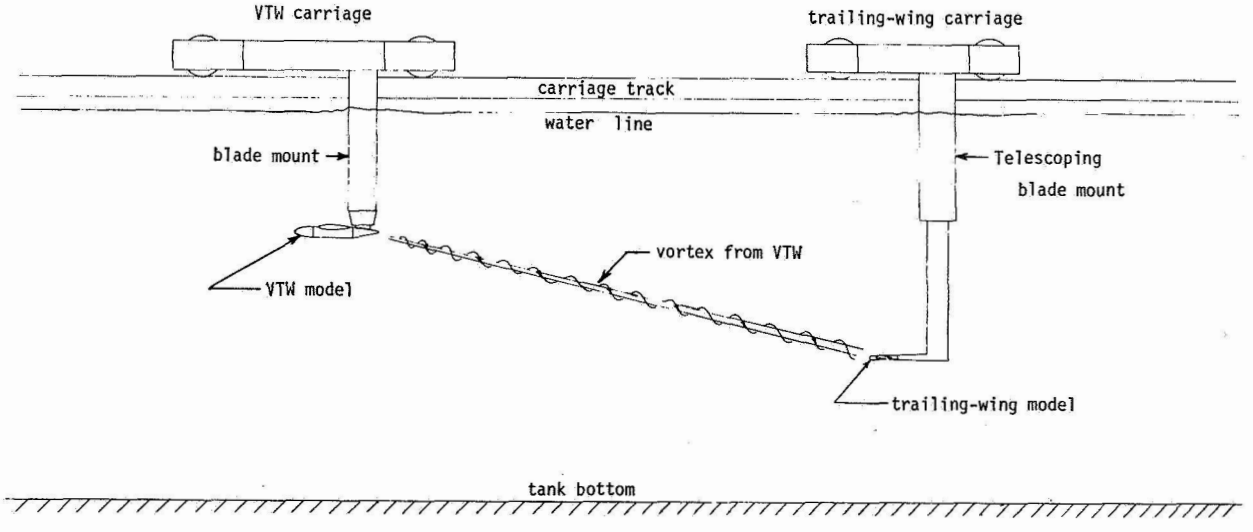

Figure 2.- Diagram of Hydronautics Ship Model Basin.

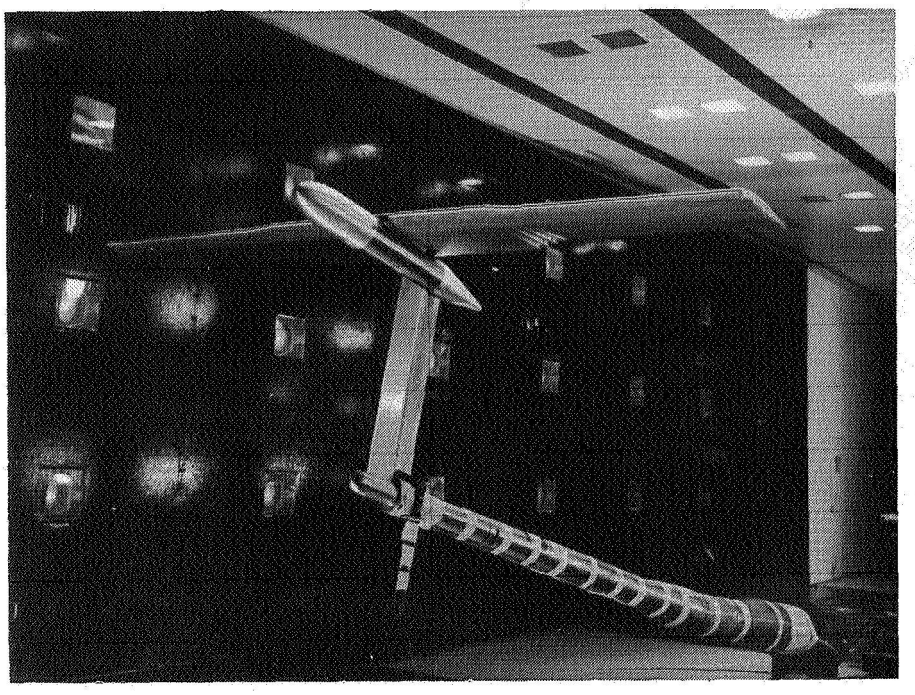

Figure 3.- Variable Twist Wing model, blade mounted in Langley V/STOl Tunnel test section.

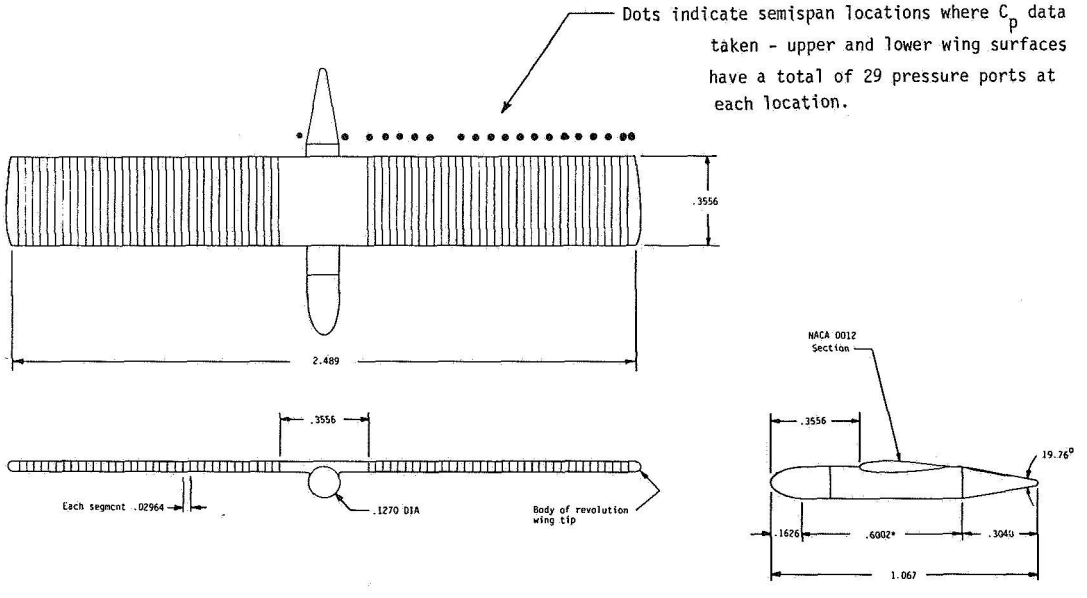

Figure 4.- Variable Twist Wing (VTW) model.

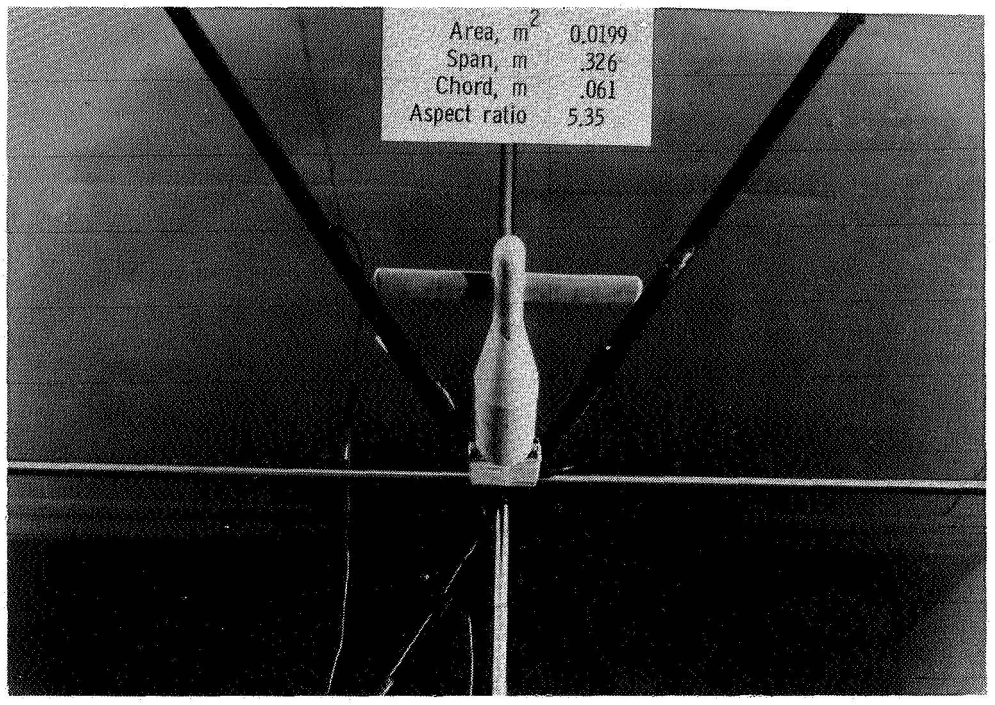

Figure 5.- Photograph and dimensions of unswept trailing-wing model on traverse mechanism. Model has NACA 0012 airfoil section.

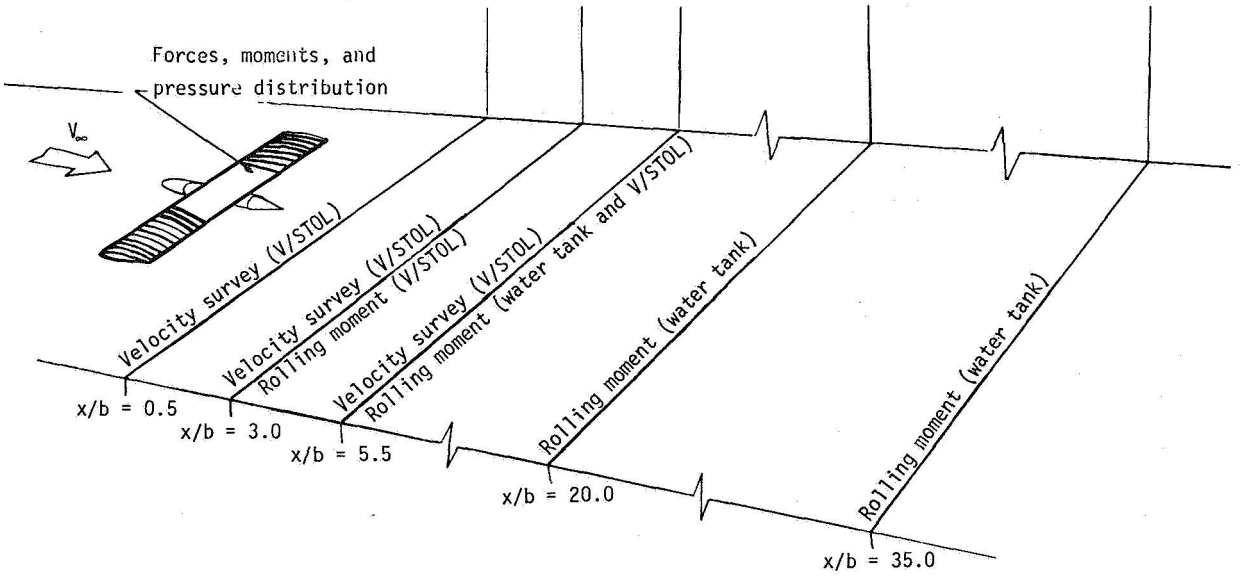

Figure 6.- Types of data taken with Variable Twist Wing model.

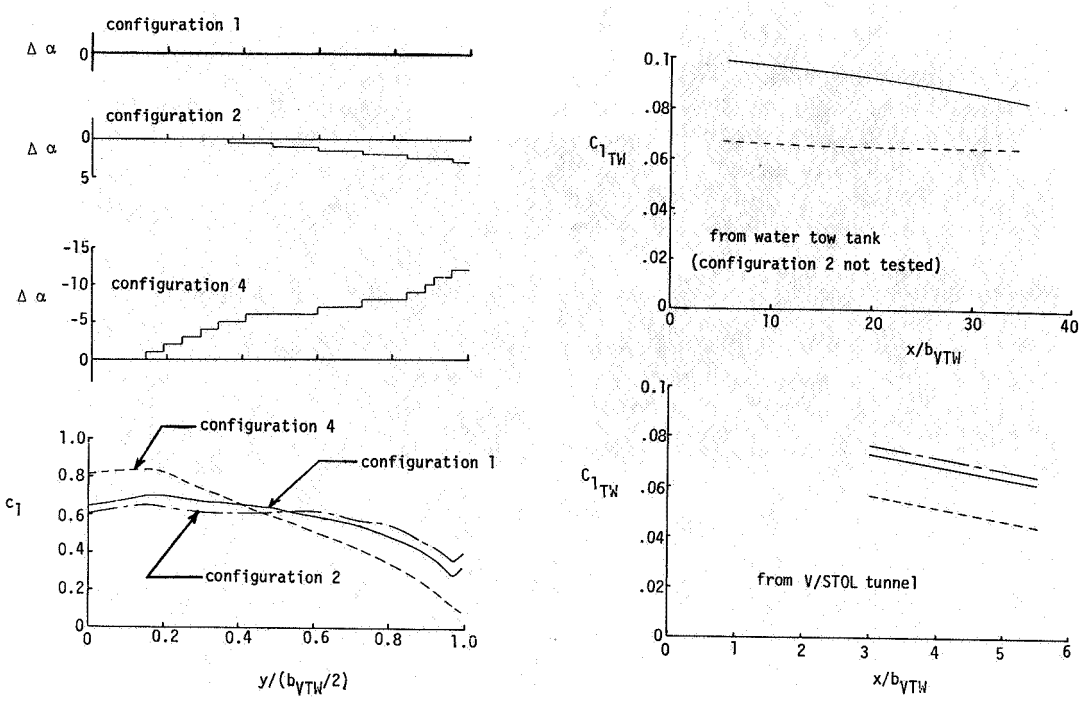

Figure 7.- Wing twist, wing loading, and trailing-wing rolling-moment comparisons for VTW configurations 1, 2, and 4.

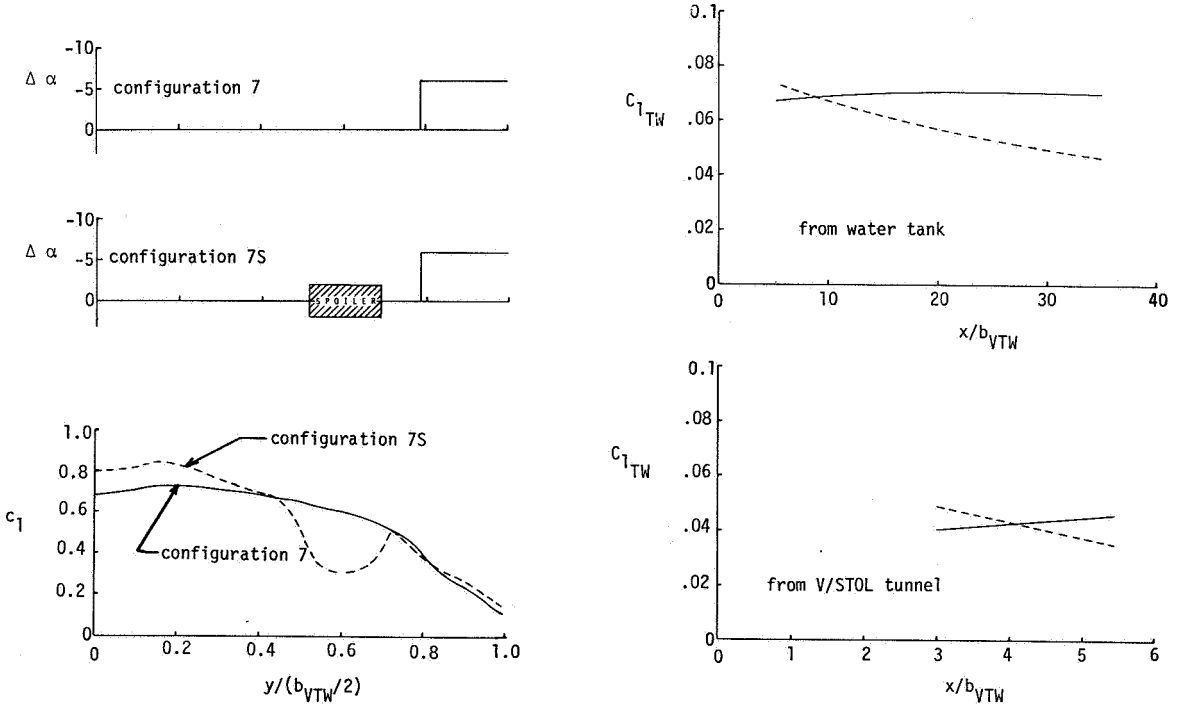

Figure 8.- Wing twist, wing loading, and trailing-wing rolling-moment comparisons for VTW configurations 7 and 7S.

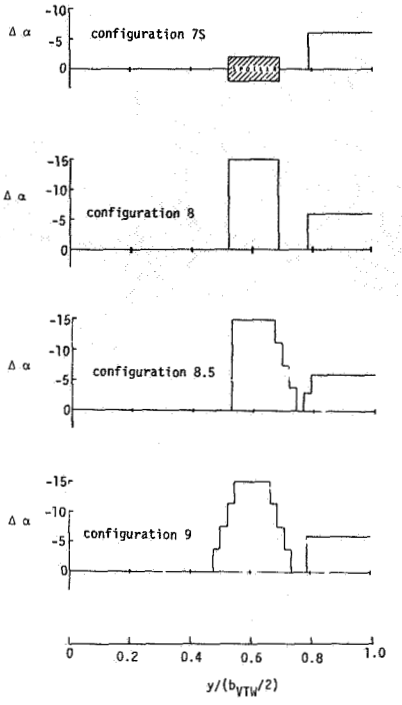

Figure 9.- Comparison of different wing twist distributions used to simulate lift distribustion attained with configuration 7S.

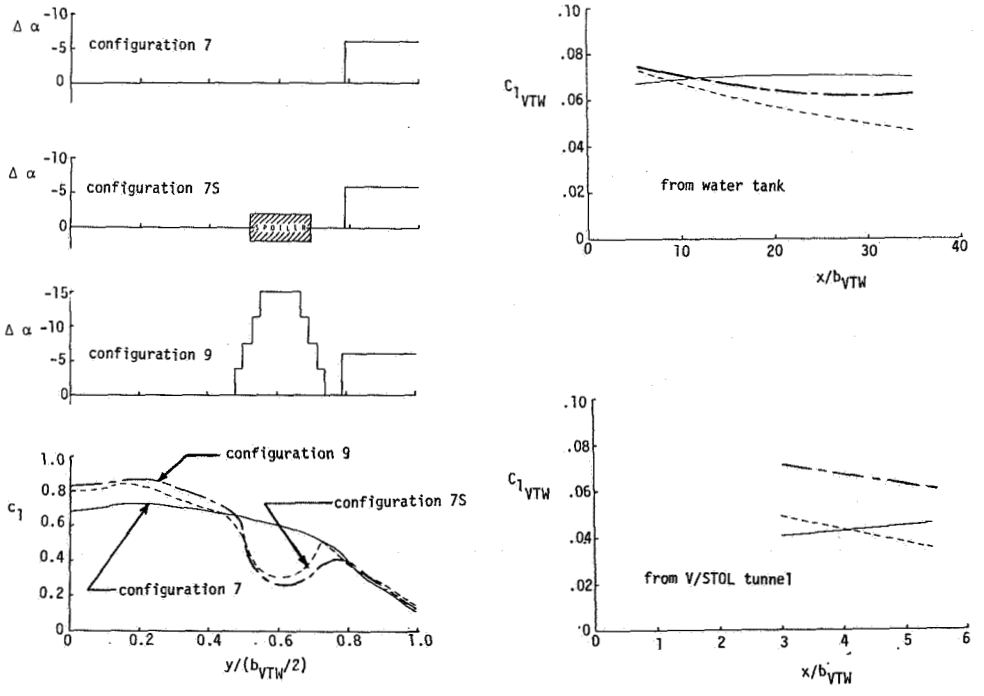

Figure 10.- Wing twist, wing loading, and trailing-wing rolling-moment comparisons for VTW configurations 7, 7S, and 9.

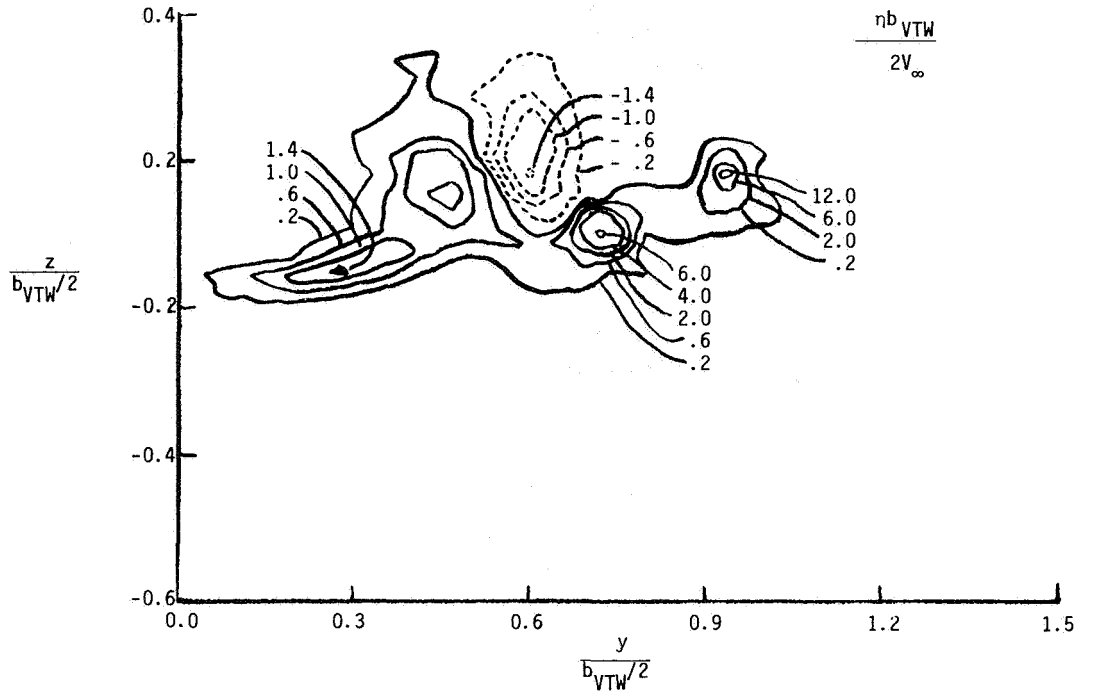

(a) $x/b_{VTW} = 0.5$.

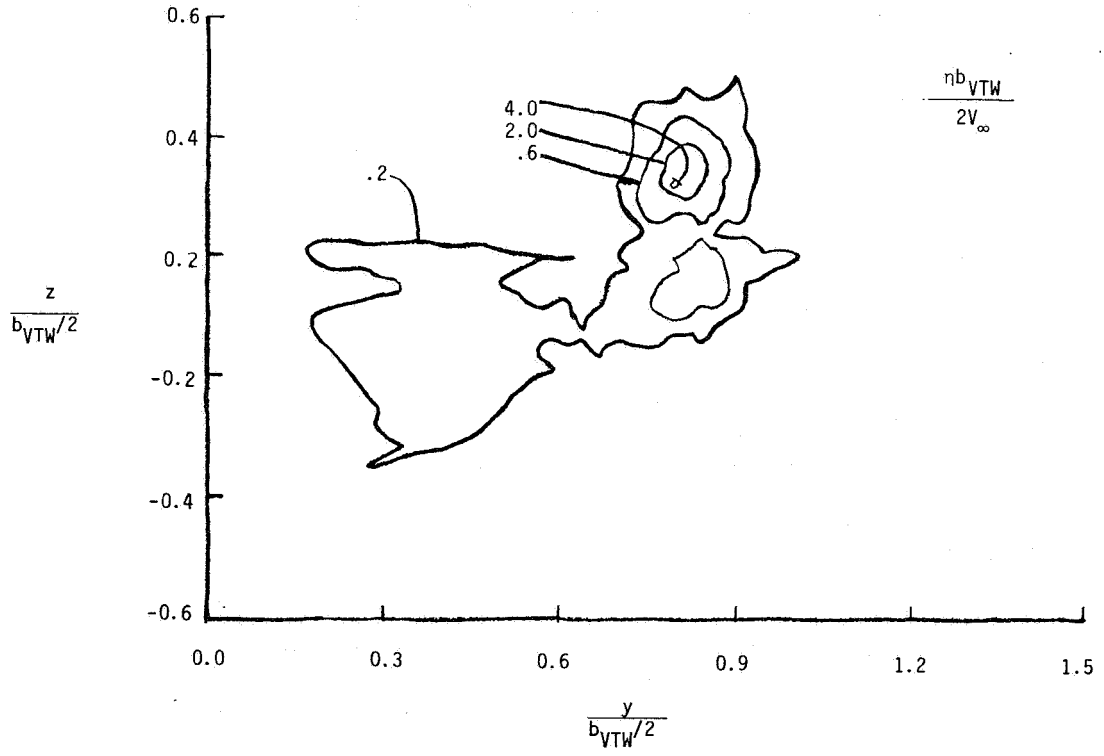

(b) $x/b_{VTW} = 3.0$.

Figure 11.- Vorticity contours measured behind configuration 7S.

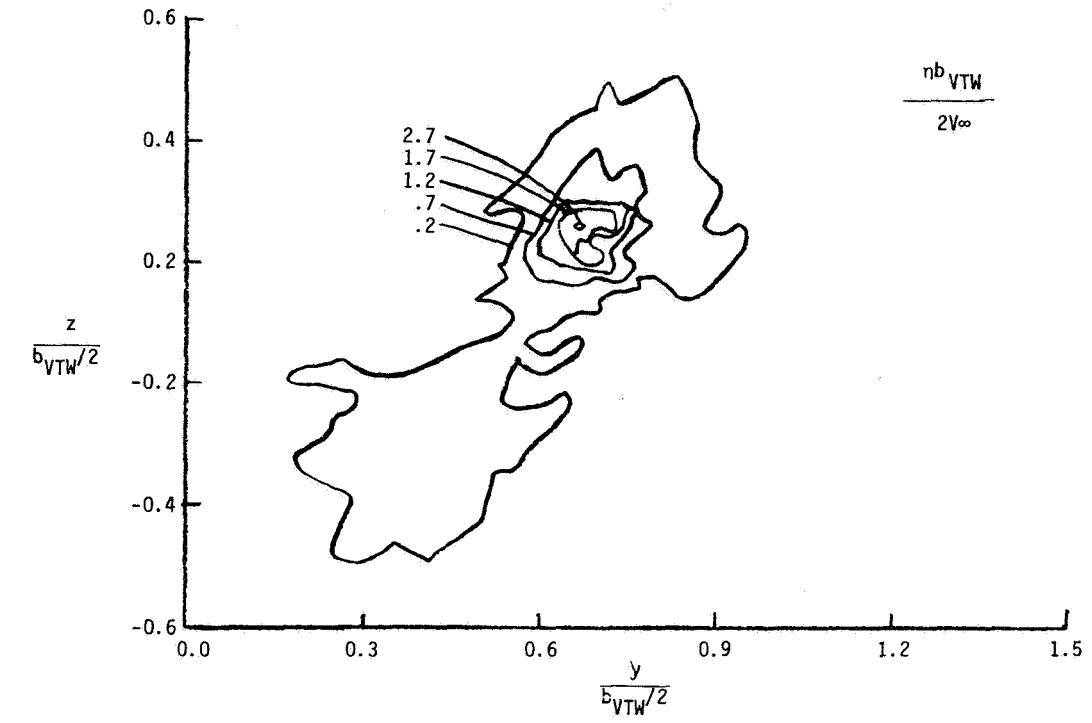

(c) $x/b_{VTW} = 5.5$.

Figure 11.- Concluded.

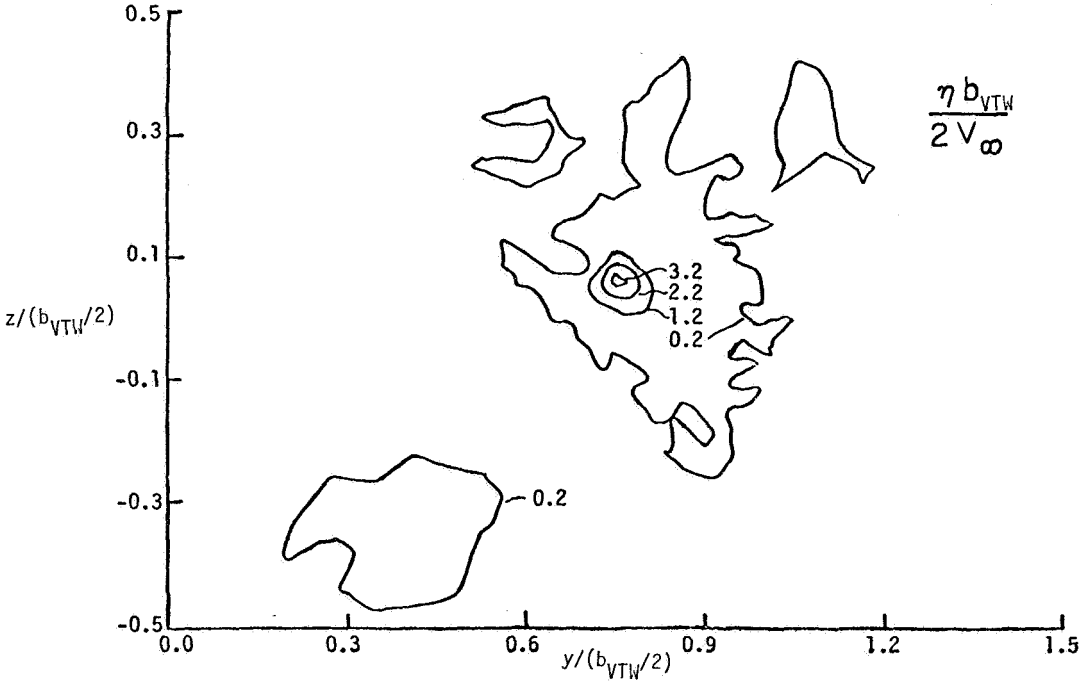

Figure 12.- Predicted vorticity contours at 5.5 spans downstream of configuration 7S.